Hindawi
Complexity
Volume 2018, Article ID 8210817, 12 pages
https://doi.org/10.1155/2018/8210817

Research Article

A Modified Time Reversal Method for Guided Wave Detection of Bolt Loosening in Simulated Thermal Protection System Panels

Guan-nan Wu,[1,2] Chao Xu,[1] Fei Du,[1] and Wei-dong Zhu[2]

[1]*School of Astronautics, Northwestern Polytechnical University, Xi'an 710072, China*
[2]*Mechanical Engineering Department, University of Maryland, Baltimore County, Baltimore, MD 21250, USA*

Correspondence should be addressed to Chao Xu; chao_xu@nwpu.edu.cn

Received 12 February 2018; Revised 7 May 2018; Accepted 13 May 2018; Published 2 July 2018

Academic Editor: Chen Lu

In this work, a modified time reversal method is proposed for guided wave detection and localizing loosened bolt in a complicated multibolt-jointed structure. Different from the traditional time reversal guided wave method, the response signal due to a tone burst input received at the healthy state is time reversed and recorded as a standard reemitting signal. In the detection process, this recorded standard signal is used for all damage cases to yield time reversal-focalized reconstruction signals. This largely improves the sensitivity of the focalized signal to damage state. In this paper, the peak amplitude of the focalized wave packet in the reconstructed signal is calculated and utilized as tightness index. By bonding PZT transducers at different joint locations inside the structure, multiple tightness indices, where each tightness index presents the correlation between the current joint condition to its healthy condition at the joint, can be obtained. To analyze a large number of tightness indices, a principle component analysis method is introduced, and a neural network-based loosening detection method is proposed. The proposed method is experimentally validated in a simulated double-layer bolt-jointed thermal protection system panel. Experimental results illustrate that the proposed method is effective to identify and localized the bolt loosening in complicated multibolt-jointed structure. The detection and identification of the location of multibolt loosening is realized.

1. Introduction

In aerospace engineering, a thermal protection system (TPS) is necessary for protecting an aerospace vehicle from harsh heating due to high reentry temperatures. It plays a critical role in keeping structural integrity and safety. A typical TPS design is a multilayer configuration, where a cover panel made of high-temperature material, such as carbon-carbon composite, is attached to the main airframe panel of the aerospace vehicle through mechanically bolted joints. The extreme thermal, vibration, and shock excitations during the flight may cause the pretightened bolts to loosen, which further cause detachment gap in a TPS. Then, hot air can penetrate through the gap and cause catastrophic results. Therefore, the detection of loosening in bolted joints plays an underlying role to ensure a TPS functionality, integrity, and reusability.

Structural health monitoring (SHM) is referred as the process of implementing a damage detection and characterization strategy for structures [1]. In the past decade, a number of SHM approaches have been developed to detect bolt loosening in TPS structures. At the early stage, the SHM methods based on experimental modal analysis were proposed to realize the objective. For example, Vandawaker et al. [2] proposed to detect damage in a TPS tile by comparing mode shapes and frequencies from healthy and damaged structures. However, since high-frequency vibration modes are difficult to obtain in practice, the modal analysis-based methods mainly rely on the low-frequency vibration modes, which only represent the properties of the whole structure. Like Todd et al. [3] pointed out an assembled structure which consists of many bolts and one or less number of loosened bolts cannot cause the whole structural properties to change significantly. Consequently, the modal analysis-based methods are relatively insensitive to detect local bolt loosening for a complicated jointed structure.

To detect local and small structural damage, a number of local SHM methods have been developed. Among them,

electromechanical impedance-based and guided wave-based methods are very popular [4, 5]. Basically, the electromechanical impedance-based method monitors variations in mechanical impedance due to damage, which is coupled with electrical impedance of a piezoelectric transducer (PZT) [6, 7]. A low-cost miniaturized impedance measurement device was developed by Peairs and Inman [8] for detection of bolt loosening. A system that includes PZTs and a wireless impedance device for data acquisition and communication was built by Mascarenas et al. [9] to detect bolt preload loss. Recently, an electromechanical impedance method for health monitoring of aircraft-bolted joints was presented by Kuznetsov et al. [10]. While the previous studies have shown the feasibility of using impedance-based approaches for detection of bolt loosening, the effective detection area of a transducer is very small and a large number of transducers are required for detecting a structure with thousands of bolts.

Guided wave-based SHM techniques have been intensively developed over the last two decades. They are very attractive and commonly utilized due to their ability to inspect a large structure over long distance with a small number of transducers. In recent years, several guided wave-based SHM methods have been proposed for bolt loosening detection. Yang and Chang [11] developed a guided wave-based method to identify bolt loosening in a TPS panel. In their study, a piezoelectric- (PZT-) embedded smart washer was developed to generate and acquire ultrasonic wave signals. The features of wave energy dissipation (WED) and specific damping capacity were extracted. However, a large number of smart washers are required in applying the detection method to a TPS with hundreds of bolts, because each bolt should be installed with a smart washer. Similar wave energy dissipation-based methods were studied by Montoya and Maji [12] and Wang et al. [13]. It is known that the nonlinear contact mechanics on the joint interface can cause nonlinear transmission of guided waves. The SHM method based on nonlinear ultrasonic wave phenomenon was proposed by Doyle et al. [14] to localize loosened bolts in a satellite panel. In their work, the acoustoelastic behavior due to the joint was used as an indicator of structural integrity. Furthermore, the feature of contact acoustic nonlinearity in bolted joints was utilized for preload monitoring [15–20]. Amerini and Meo [15] studied both linear and nonlinear ultrasonic methods and proposed several tightening state indices, including the first-order acoustic moment, high-harmonic generation, and sideband modulation indices. Bao et al. [16] established a nonlinear contact element model to simulate the strip lap joint specimen. On this basis, the high-harmonic generation-based index was studied by Shen et al. [17]. After that, Zhang et al. [18] proposed to use subharmonic resonance to detect bolt looseness, and Zhou et al. [19] utilized nonlinear-modulation method to detect bolt looseness in frame structure. Zhang et al. [20] carried out a comparative study of the WED-based method and the vibroacoustic modulation-based method and found that the sensitivity of WED-based methods is closely related to the wave energy transmitted across joints.

In recent years, new guided wave detection methods based on the time reversal principle in modern acoustics have been developed and the effectiveness was demonstrated. Fundamentally, the time reversal concept lies in reconstruction of an input signal at an excitation point, while a response signal measured at another point is reemitted to the original excitation point after being reversed in time domain, taking into account that there is no damage in the wave path. As a result, changes between the reconstructed signal and the input signal can be inferred as presence of damage in the wave path. Wang et al. [21] carried out an experimental work to study the applicability of the time reversal concept to guided waves in plates. Then, Park et al. [22] utilized the time reversal technique to improve the detect ability of local defects in composite plate. A detailed theoretical investigation on the effect of multimodel and reflections on time reversal progress was given in [23]. It was pointed out that narrowband input signal can enhance time reversal progress. In recent years, the technique of time reversal guided wave SHM has been applied to a variety of structures, such as metallic plates [24], composite plates [25], and rebar-reinforced concrete beams [26]. Mustapha and Ye proposed a very effective and innovative time reversal-based imaging algorithm to detect debonding in sandwich composite plates [27] and then extended it to detect multiple debonding in complex tapered composite sandwich panels [28]. However, the time reversal guided wave method has not been widely used for detection of bolt loosening, except the works done by Tao et al. [29] and Parvasi et al. [30], where only very simple single bolt lap-jointed structures were considered. In their work, the aim is to identify the preload loss in single bolt. The problem of detection of loosening in a multibolt-jointed structure was not considered.

In this paper, a modified time reversal (MTR) guided wave method is proposed to detect bolt loosening in TPS panels. The conventional time reversal process is modified, and a new implemented process is proposed to localize loosening bolts in a complicated multibolt-jointed structure. In the proposed method, a standard remitted signal which recorded for a nominal healthy structure is used for all damage cases. The peak amplitude of the refocused wave packet obtained by the MTR method is normalized and utilized as the tightness index. By bonding PZT sensors at different joint locations inside the structure, multiple tightness indices can be obtained, where each tightness index presents the correlation between the current joint condition to its healthy condition at the joint. To analyze a large number of tightness indices, a principle component analysis method is introduced, and a neural network-based loosening detection method is proposed. The feasibility and effectiveness of the proposed method to identify and localize bolt loosening is experimentally investigated in a simulated TPS structure.

2. Theory Background

2.1. The Conventional Time Reversal Guided Wave Method. Figure 1 shows the work principle of the conventional time reversal guided wave method in a simple lap joint. First, a

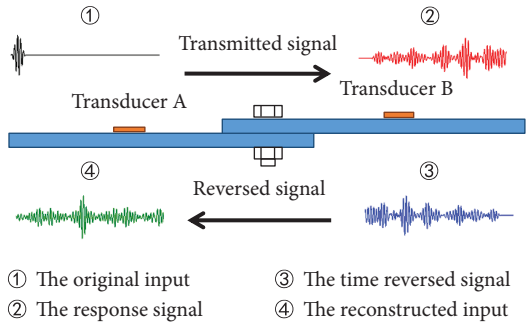

Figure 1: Illustration of the time reversal principle in a lap joint.

tone burst input $e(t)$ is applied to transducer A, which acts as an actuator and activates wave propagation in the structure. A wave response signal $u(t)$ is captured by the transducer B. The response signal at the transducer B can be defined as

$$u(t) = h(t) * e(t), \tag{1}$$

where $h(t)$ is the impulse response function (IRF) of the structure between points A and B; $*$ denotes the convolution. After that, the recorded response signal is reversed in time domain before reemitted at transducer B. Thus, the reemitted signal is

$$u(-t) = h(-t) * e(-t). \tag{2}$$

After the signal is reversed in time domain, the wave packets that arrive at transducer B early will be reemitted late, and the wave packets that arrive at transducer B late will be reemitted early. Therefore, wave packets in the time-reversed signal arrive at transducer A at the same time and overlap to a focalized wave packet. Note that, in practical applications, the reversed signal is amplified before feeding it into PZT B. The reconstructed signal received at the transducer A can be written as

$$\begin{aligned} s(t) &= h(t) * u(-t) = h(t) * h(-t) * e(-t) \\ &= e(-t) * \int_{-\infty}^{+\infty} h(\tau)h(\tau - t)\mathrm{d}\tau = e(-t) * R_{11}(t), \end{aligned} \tag{3}$$

where $R_{11}(t)$ is a autocorrelation function and also called the time reversal operator. $R_{11}(t)$ gets its maximum value at time point $t = 0$ and is equal to the energy of IRF of the structure between points A and B. It is noted that the energy of IRF is decided by the wave energy transmits through the joint interface. Bolt loosening causes the decrease of contact area and consequently transmitting wave energy and the IRF energy decreases. Thus, the peak amplitude of reconstructed signal $s(t)$ is proportional to the IRF energy, and the peak amplitude of $s(t)$ can be extracted as a tightness index (TI) to detect bolt loosening.

This principle is used by Tao et al. [29] and Parvasi et al. [30] for detecting preload loss in a single bolted lap joint. However, the results show that a saturation phenomenon of the TI happens when the preload reaches to a critical value [29, 30]. The reason is that the feature of peak amplitude is related to the IRF and the wave energy transmitted across joint, which are determined by the contact area. When the preload is high, the contact area changes very little due to the change of preload. Thus, in this situation, the IRF nearly holds constant. This causes the conventional time reversal guided method which has a low sensitivity at the early stage of loosening.

2.2. The Modified Time Reversal Guided Wave Method. The basic idea of the MTR method is to introduce a "standard" reemitted signal (SRS) for all damage cases, where damage is referred to bolt loosening in this work. As shown in Figure 2, the time-reversed reemitted signal (the symbol ③ signal in Figure 1) recorded at the nominal healthy structure is chosen as the "standard" reemitted signal for all damage cases. When the SRS is reemitted back to the structure, damage affects the reconstructed signal in extensive patterns comparing to the conventional time reversal method. Thus, additional damage information that can be extracted to reveal the extent of damage is contained in the reconstructed signal. The detailed explanation of the proposed modified method is presented below.

Fundamentally, when a SRS is reemitted back to the structure, if the bolt in the wave path is not loosened, which means the structure can be regarded as the same as the nominal healthy structure, the MTR is therefore equal to the TR method. The velocities for every wave packet in the SRS keep the same and a focalized wave packet can be obtained by the backward travelling of SRS, due to the in-phase overlapping of wave packets in the SRS. However, if the bolt in the wave path is loosened, the wave velocity for each wave packet may also be changed. According to Zagrai et al. [31], the main reason of the change of wave velocity is due to acoustoelastic effect. With the change of bolt preload, the static stress level changes and the wave speed of the transmitted guided wave signals changes. Therefore, the in-phase overlapping of wave packets in the SRS cannot be realized to a focalized wave packet. This indicates that in the MTR method, not only the transmitted wave energy is related to the peak amplitude of the reconstructed signal, but also the impaired focalizing ability of SRS can cause the decrease of the peak amplitude.

If the IRF of the healthy structure between a actuator and a sensor is $h_1(t)$, therefore, as the same as (1), the "standard" reemitted signal can be written as

$$u_{\text{stand}}(-t) = h_1(-t) * e(-t). \tag{4}$$

This signal is recorded and used for all damage cases. If there exists damage in the wave path, it is obvious the IRF changes. It is assumed that the IRF of the damaged structure is $h_2(t)$, and then the reconstructed signal $s_2(t)$ due to the SRS can be obtained, defined as

$$\begin{aligned} s_2(t) &= h_2(t) * u_{\text{stand}}(-t) = h_2(t) * h_1(-t) * e(-t) \\ &= e(-t) * \int_{-\infty}^{+\infty} h_1(\tau)h_2(\tau - t)\mathrm{d}\tau = e(-t) * R_{21}(t), \end{aligned} \tag{5}$$

where $R_{21}(t)$ is a cross-correlation function of $h_1(t)$ and $h_2(t)$ and represents the degree of the correlation of $h_1(t)$ and

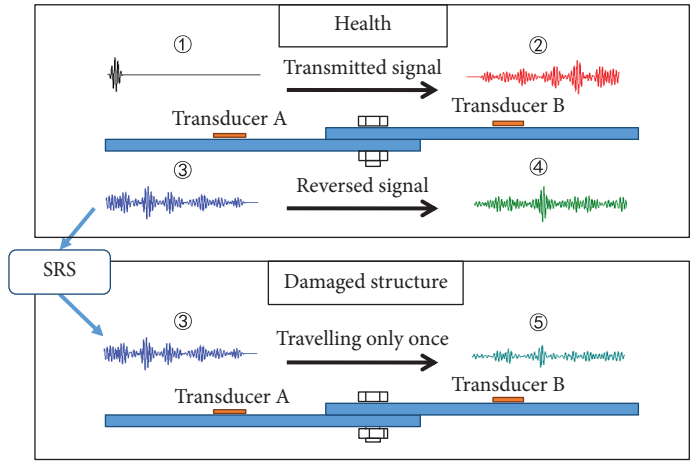

Figure 2: A schematic of the proposed method for bolt loosening detection.

$h_2(t)$. R_{21} gets its maximum value at the time instant $t = \Delta t$. Comparing (5) to (3), it can be seen that the MTR method actually modifies the time reversal operator. In the conventional time reversal method, the autocorrelation function of the IRF is used, while in the modified time reversal method, by introducing a reference IRF, the cross-correlation function is used as the time reversal operator. Meanwhile, it can be found that in (5), similar to (3), the peak amplitude of the focalized wave packet is proportional to the maximum value of R_{21}. Therefore, the principle of the proposed method is to change the time reversal operator from the autocorrelation function of structural states to the cross-correlation function of structural states.

It should be noted that in the conventional time reversal method, for any signal path, both transducers need to work as actuators and sensors. This often means a large number of hardware, such as PZT amplifier and wiring are required. In [25], a simplified time reversal method is proposed, which can largely reduce the hardware requirement by using only one transducer A to actuate signals and another transducer B to act as a sensor for a signal path. The underlying reason is that the impulse response function (IRF) of the structure from point A to B is assumed the same as that from point B to A. In this paper, the same simplified technique is used to reduce hardware requirement and experimental cost.

2.3. Loosening Localization Method for Multibolt Structures. It is noted that the above-proposed principle uses a single bolt loosening detection problem as an example. However, the proposed method can be easily extended to a multibolt structure. In this paper, the aim is to detect the loosening location for a multibolt TPS structure. To this end, each joint with attached bolts is considered as a possible loosening location. At each possible loosening location, a PZT sensor is bonded to act as a wave signal receiver. In addition, a PZT transducer boned at the central location of bottom panel is used to generate wave signal to sensors. The detailed sensor configuration is given in the next section.

In this paper, the peak amplitude of the reconstructed focalized wave packet is extracted as a TI for detection of bolt loosening in a multibolt-jointed TPS structure. The TI can be written as

$$\mathrm{TI}_i = \frac{A_{ij}}{A_{i0}}, \tag{6}$$

where A_{ij} is the peak amplitude of reconstructed signal received by sensor i at the current structure, and A_{i0} is the peak amplitude received by sensor i at the healthy structure. By installing PZT sensors around every possible loosening bolts, predictive variables TI_is can be defined. Each TI_i represents the correlation coefficient of a structural state of a joint to its healthy state. For instance, bolt loosening happening at joint 1 changes the IRF of actuator to sensor 1 significantly; according to (5) and (6), the corresponding TI_1 is therefore significantly decreased. On the other hand, the loosening at joint 1 has less effect to the IRF of actuator to sensor 2 which is far from joint 1. Hence, the TI_2 corresponding to sensor 2 shows a smaller change than TI_1 when loosening occurs at joint 1. Depending on this feature, the bolt loosening in the structure can be detected by using predictive variables TI_is.

To implement the proposed MTR method, each bolt joint location needs one sensor to form a signal path. Hence, in real application, a great number of transducers may be needed, and a lot of variables need to be processed, correspondingly. However, too many predictive variables cause the difficulty in the visual description of detection results. Therefore, it is important to keep the independence of each predictive variable for the proposed method. In this paper, dimension reduction of predictive variables TI_is before the establishment of damage index database is performed. The principal component analysis (PCA) [32] is used for dimension reduction of TI_is. First, TI_is should be scandalized to mean equals to zero and the standard deviation equals to one. Assuming TI_i is a $n \times 1$ vector and n is the number of data. $\mathbf{D}$ is the $n \times m$ matrix composed by TI_is, where m is the number of the predictive variable. Then, the normalized matrix $\mathbf{X}$ can be obtained by

$$\mathbf{X} = \left(\mathbf{V}^{1/2}\right)^{-1}(\mathbf{D} - \mu), \tag{7}$$

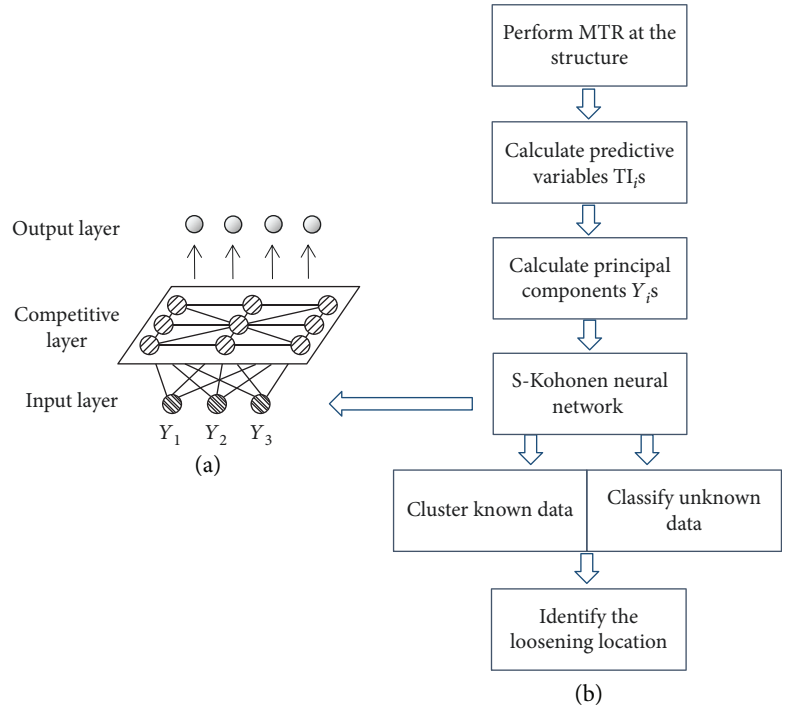

Figure 3: The schematic of the proposed method: (a) the topological structure of S-Kohonen network and (b) the flow chart of the loosening detection process.

where index "−1" means calculating inverse, μ is the means of $\mathbf{D}$, and $\mathbf{V}^{1/2}$ is a $m \times m$ matrix of standard deviation, defined as

$$\mathbf{V}^{1/2} = \begin{bmatrix} \sigma_{11} & 0 & \dots & 0 \\ 0 & \sigma_{22} & \dots & 0 \\ \vdots & \vdots & \ddots & \vdots \\ 0 & 0 & \dots & \sigma_{\mathrm{mm}} \end{bmatrix}, \quad (8)$$

where σ_{ii} is the standard deviation of TI_i. Calculating the covariance matrix $\mathrm{Cov}(\mathbf{X})$ of $\mathbf{X}$, and we can get the eigenvalues and eigenvectors $(\lambda_1, e_1), (\lambda_2, e_2), \dots, (\lambda_{\mathrm{m}}, e_{\mathrm{m}})$ of $\mathrm{Cov}(\mathbf{X})$. Then, the number i principal component Y_i can be obtained by

$$Y_i = (\mathrm{TI}_1, \mathrm{TI}_2, \dots, \mathrm{TI}_{\mathrm{m}}) e_i. \quad (9)$$

The number of principal component can be determined by the data variation ratio that the obtained Y_i can explain. Generally, 90% of data variation should be explained by the k principal components, that is,

$$\sum_{i=1}^{k} a_i \geq 90\%, \quad (10)$$

where a_i is the data variation explained by Y_i and $a_i = \lambda_i / m$.

Finally, the S-Kohonen neural network [33] is used in this work for clustering analysis of the known data and classifying of the unknown data. The S-Kohonen neural network is an extended Kohonen neural network (KNN) that contains an added output layer. As shown in Figure 3(a), a typical KNN contains an input layer and a competitive layer, the node number of input layer equals to the predictive variables, and the competitive layer is a 2D array that usually contains much more nodes than the target variables. Furthermore, the S-Kohonen network has an added output layer after the competitive layer to connect target variables directly to the clustering result. By performing the above steps, a loosening detection flow can be built, as shown in Figure 3(b).

3. Experimental Study

3.1. The Simulated TPS Structure. As shown in Figure 4, a simulated multibolt-jointed TPS structure is considered for validating the proposed MTR method. A Q235 steel thin plate simulating the cover panel is attached to a Q235 steel thin base plate to simulate the airframe panel via four steel brackets. M6 bolts are used as fasteners. The dimension of the base plane is 450 mm × 385 mm × 3 mm and the upper plane is 335 mm × 335 mm × 3 mm. PZT patches are used to actuate and receive wave signals. One PZT actuator is bonded on the center of the base plate, and each bracket is bonded with one sensor. The PZT sensor location and the bolt numbers are shown in Figure 4.

Considering the allowable tensile load of M6 bolt and the yielding strength of Q235 steel, 10 N•m is selected as the standard bolt torque. For each bracket, totally, 6 bolt loosening cases are taken into account as shown in Table 1. During the experiments, each bolt loosening case is repeated four times to get reliable results. In this work, the bolt loosening means a totally loose condition. In each bolt loosening detection experiment, the TPS panel specimen is assembled

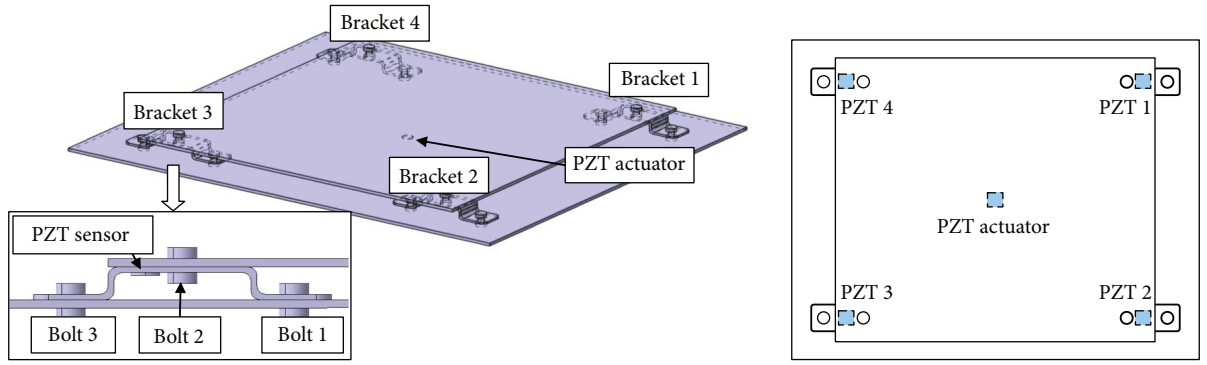

Figure 4: A schematic of the simulated PTS panel: (a) the simulated PTS panel and its brackets and (b) relative locations of the PZT transmitters.

Table 1: Bolt loosening conditions for each bracket.

Case number	1	2	3	4	5	6
Loosened bolt	Bolt 1	Bolt 2	Bolt 3	Bolts 1 and 2	Bolts 2 and 3	Bolts 1 and 3

to the normal tightening condition firstly, and then it is adjusted to a bolt loosening case by loosening corresponding bolts. A standard assembly sequence is regulated to guarantee experimentally repeatability. Each bolt is tightened to 70% standard torque firstly and then tightened to 100% in sequence to prevent unnecessary internal stress.

3.2. Experimental Setup. Figure 5 gives the experimental setup. The multifunction data acquisition (DAQ) system NI USB-6366 is used to generate and receive guided wave signals. Before the input signal is sent to PZT actuator, a signal amplifier PINTEK HA-400 is used to amplify the signal amplitude to 50 Vpp (peak to peak). A LabVIEW program is coded and runs on the computer to control the DAQ system. In addition, the structure is placed on a foam support.

A 5-cycle tone burst is used as the original input of MTR process. The central frequency of the input is chosen as 150 kHz based on the group velocity dispersion plot of 3 mm steel plate, as shown in Figure 6. It can be seen that at 150 kHz, only the first S_0 symmetrical mode and antisymmetrical A_0 mode are generated, and the velocity dispersion of these modes is minimized. Response signals of the tone burst input at each sensor in the healthy structure are recorded. After reversed in time domain, they are saved as SRSs. The generated and recorded signals in the MTR method for the healthy state are shown in Figure 7. To reduce the effect of noise, each recorded signal is the average of 32 measurements. Moreover, a high-pass filter is used to cut off the low-frequency noise; the low-pass cutoff is set to 10 kHz. It can be clearly found that a focalized wave packet occurs in the reconstructed signal.

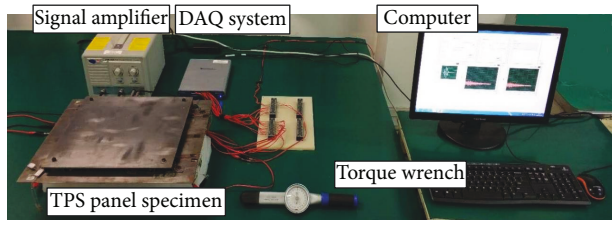

Figure 5: The experimental platform.

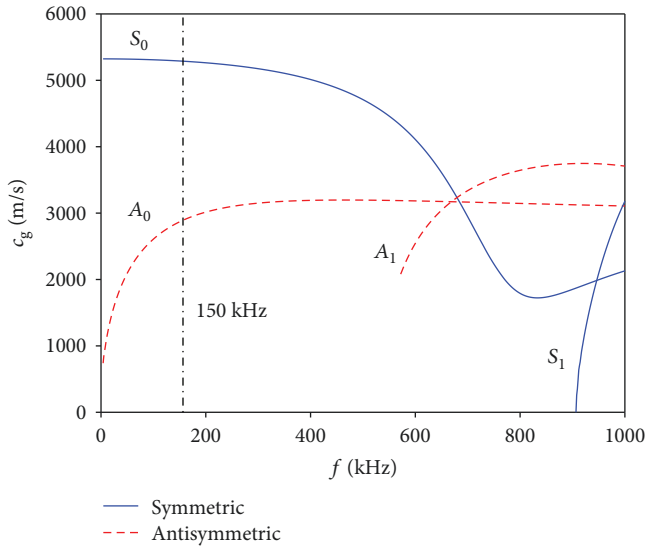

Figure 6: The group velocity dispersion plot of 3 mm Q235 steel plate.

4. Results and Discussion

4.1. Validating the Modified Time Reversal Process. By implementing the proposed time reversal method, the reconstructed signals recorded at each bracket sensor for the healthy structure are given in Figure 8(a). It can be seen for the healthy state that each sensor received a clear

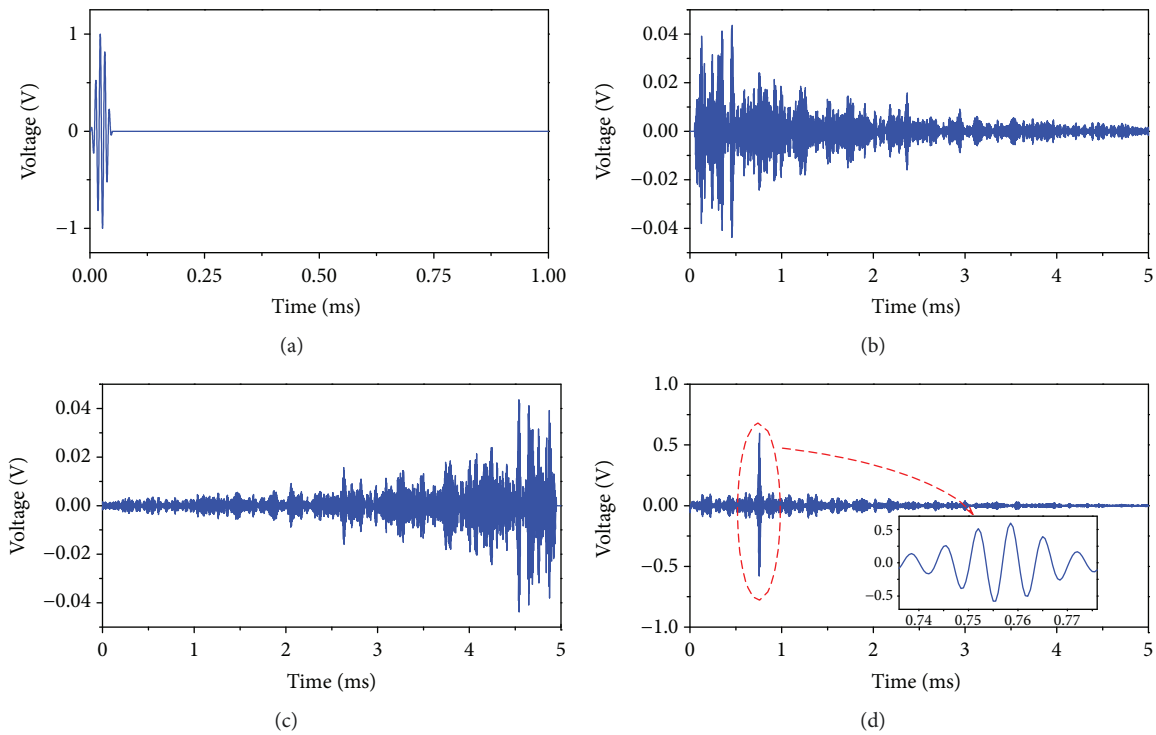

Figure 7: Input/output signals of the time reversal process: (a) the tone burst input, (b) response signal due to the tone burst input, (c) the time-reversed reemitting signal, and (d) the reconstructed signal received at healthy structure.

reconstructed signal with a focalized wave packet. This result corresponds with the conventional time reversal guided wave method. However, it can be found that the peak amplitudes of the focalized wave packet for each sensor are slightly different. This is due to the structural assembly error and the deviation of bonding condition of PZT patches.

The reconstructed signals in Figure 8(b) were normalized by the corresponding reconstructed signals for the healthy structure. Then, the peak amplitudes of the reconstructed signals for the healthy structure were normalized to 1. Figure 8(b) shows the comparisons of normalized peak amplitudes for damaged and healthy structures at different PZT locations. It is found that a focalized wave packet still exists in the reconstructed signal for each sensor, but the peak amplitude of reconstructed wave packet at each sensor changes obviously. Since the loosening of bolt 2 in bracket 2 has changed the wave propagation behavior of the whole structure significantly, the peak amplitude of each PZT patch is affected by different extents. It can be seen in Figure 8(b) that the peak amplitude decreases the largest at the PZT patch bonded on bracket 2 compared to the other three results.

4.2. Predictive Variables TI_is. The predictive variables TI_is for each bracket at different bolt loosening cases are calculated and shown in Figure 9. First, it can be seen that in each bolt loosening case, each TI_i is less than 1, and the loosening bracket corresponding TI_i is smaller than the other TI_is. Therefore, based on TI_is, the bolt loosening location can be identified by directly comparing the values of predictive variable. Second, the robustness of the MTR method is examined by three repeating experiments at each bracket. It can be seen that at each bolt loosening case, the predictive variable TI_i at each bracket appears similar character, and from three repeating experiments, good repeatability of the measurement can be observed.

In addition, it can be seen that the mismatched TI_is of the loosening bracket is nearly unchanged at each case, but the corresponding TI_i changes with the change of case number. On the one hand, comparing the results of case 1/2/3, it can be found that the loosening of bolt 3 has the most significant influence to the corresponding TI_i. On the other hand, the change of TI_i becomes more distinct with the increase of the number of loosening bolt. Checking on Figure 4, it can be found that the bolt 1 is the farthest bolt to the PZT sensor, and bolt 2 is the nearest one. Since the actuator PZT patch is bonded on the base plate, the loosening of bolt 1 and bolt 3 has direct influence to the wave propagation path, comparing to bolt 2 which connects the bracket with the cover plate. Overall, considering these factors, the reason of why bolt 3 has the most significant influence to TI_i can be explained: (1) the loosening of bolt 1 and bolt 3 can directly affect the wave propagation path, and (2) bolt 3 is more closer to the PZT sensor than bolt 1.

4.3. Clustering Results. The PCA of TI_is is performed in this step. The correlation of TI_is is shown in Figure 10, and it can be seen that predictive variables TI_1, TI_2, TI_3, and TI_4 show the same correlation with each other. For instance, the values of TI_1 and TI_2 are high when the bolt loosening happens at bracket 3 and bracket 4, and when it happens at

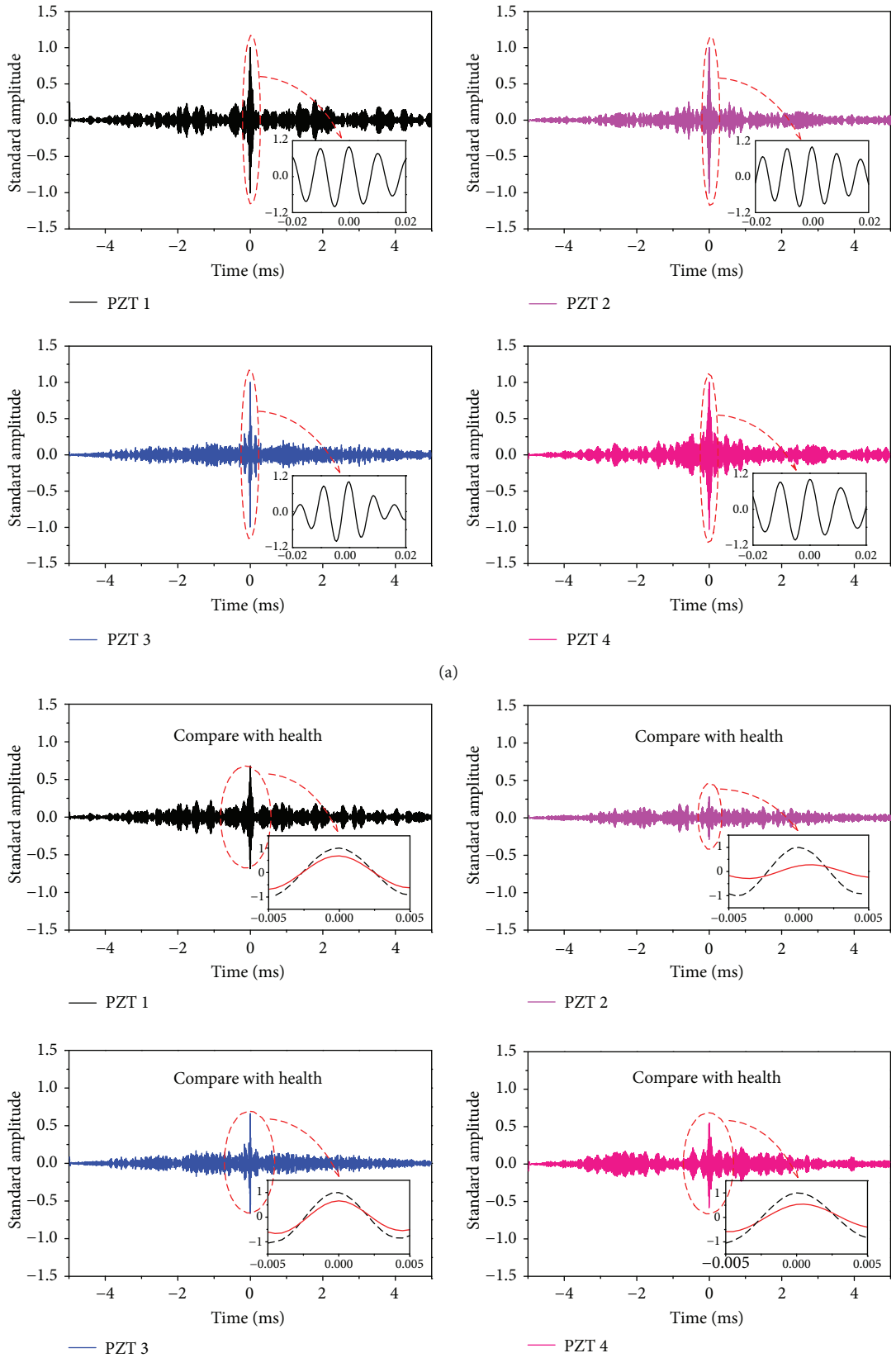

Figure 8: Experimental results using the proposed method: (a) normalized reconstructed signals for healthy structure and (b) reconstructed signals for damaged structure with joint loosening at the bracket 2.

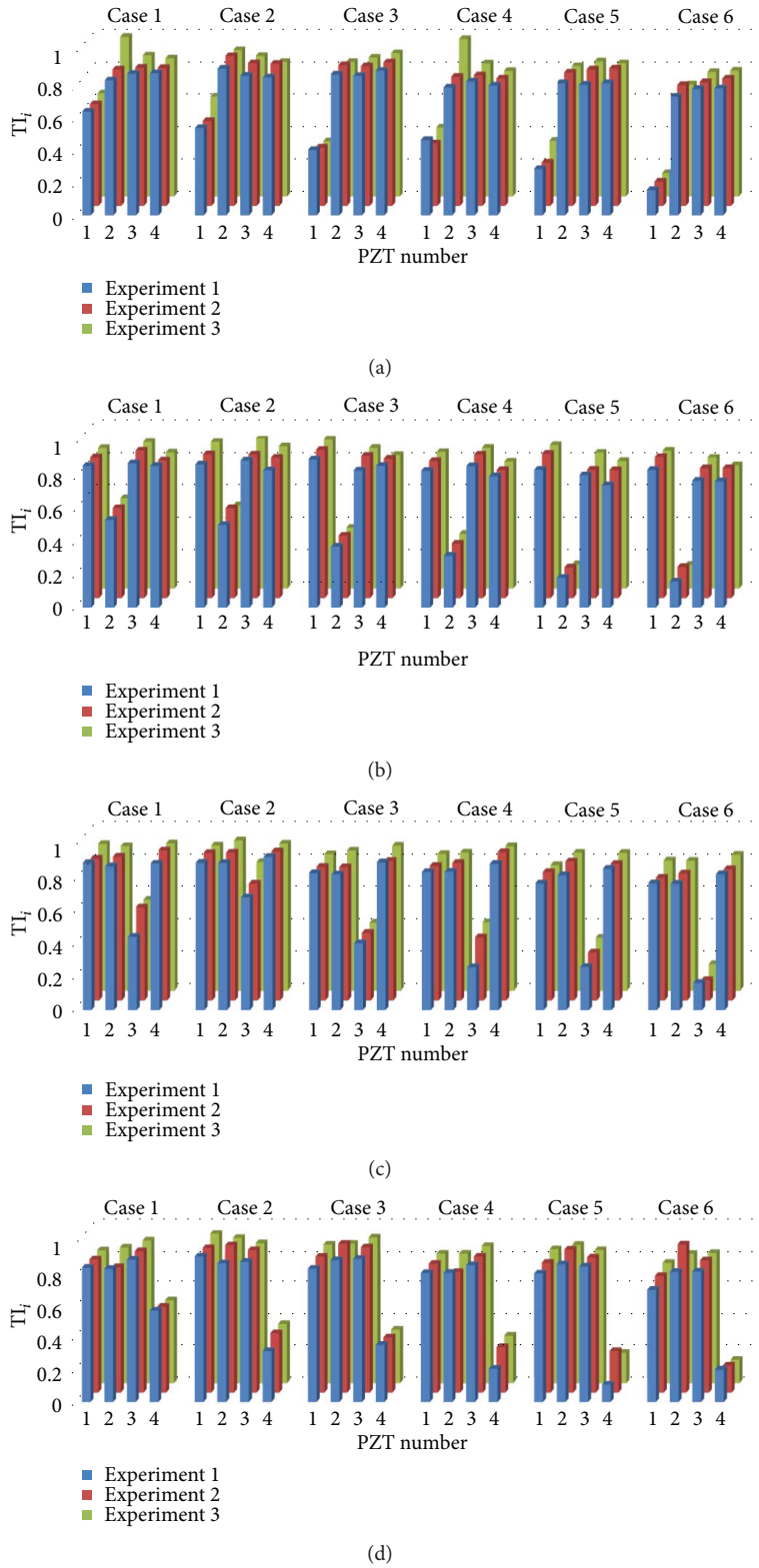

FIGURE 9: The predictive variables TI_is at different bolt loosening cases: (a) results of bracket 1, (b) results of bracket 2, (c) results of bracket 3, and (d) results of bracket 4.

bracket 1 and bracket 2, TI_1 and TI_2 get a low value, respectively. The scatter diagram of TI_1 and TI_2 appears a curvilinear correlation with the loosening at different positions. Furthermore, it can be found that this relationship is kept in the correlation of other predictive variables. Since a same curvilinear correlation is found between any two TI_is, it

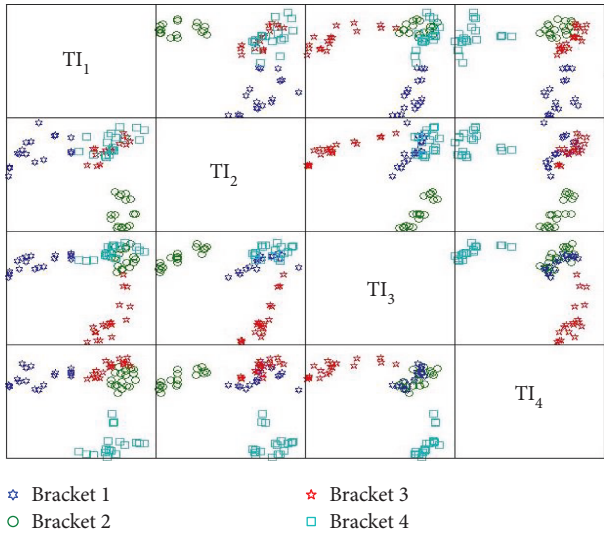

Figure 10: The correlations of predictive variables TI_is; each symbol represents a bracket number where bolt loosening happens.

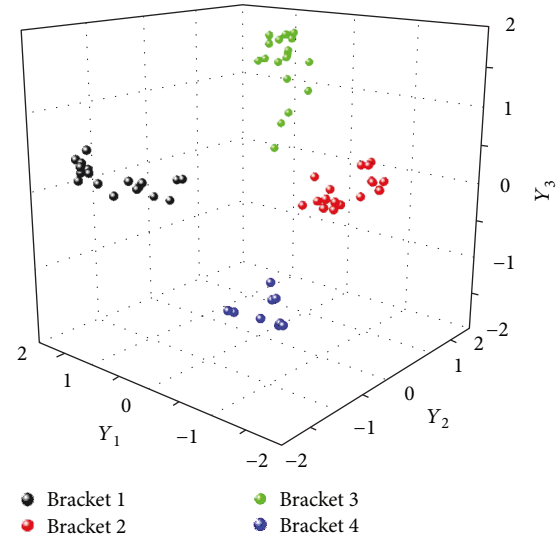

Figure 11: The 3D scatter plot of Y_1, Y_2, and Y_3.

indicates that the PCA method can be performed properly to extract principal components.

This study got 96 TI_is from 4 repeating experiments of 6 bolt loosening cases at 4 brackets, respectively. The 72 data from the first 3 times repeating experiments were used to establish a database, and the last 24 data were utilized as test. The PCA for the 72 data was performed, and the covariance matrix $\mathrm{Cov}(\mathbf{X})$ was calculated. Then, the eigenvalues and eigenvectors of $\mathrm{Cov}(\mathbf{X})$ were calculated as $\lambda_1 = 1.3938$, $\lambda_2 = 1.2234$, $\lambda_3 = 0.9615$, and $\lambda_4 = 0.4213$. Based on (10), it can be found that when $k = 3$, the principal components can explain 89.47% of the data variation. A 3D scatter plot of principal components Y_1, Y_2, and Y_3 is shown in Figure 11; it can be found that the data at the same loosened bracket is close to each other and the distance of data from different loosening brackets is large. This distribution of data guarantees the accuracy of the clustering analysis and the possibility for bolt loosening locating.

4.4. Tests of the Loosening Detection Database. Figure 12 shows the distribution of winning nodes at the competitive layer of the 72 Y_is data in one running result of S-Kohonen neural network. Accordingly, the node number of input layer is 3, and the node number of competitive layer is $4 \times 4 = 16$. The learning rate is set to [0.01, 0.1], and the learning diameter is set to [0.4, 2]; number of cycles is 1000. In Figure 12, the symbol represents bolt loosening cases at bracket 1, the symbol ② represents bolt loosening cases at bracket 2, and the rest can be done in the same manner. The blank represents the node not belonging to any cluster. It can be seen that the winning nodes distribute as blocks; the effect of clustering analysis is good.

Based on (9), the last 24 TI_is data can be transferred to Y_is. The classifying results of S-Kohonen network is shown in Figure 13. The node number of the output layer is 4, and learning rate between the output layer and the competitive layer is [0.5, 1]. It can be seen that all of the

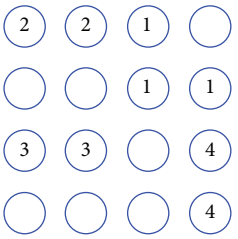

Figure 12: The distribution of winning nodes at the competitive layer.

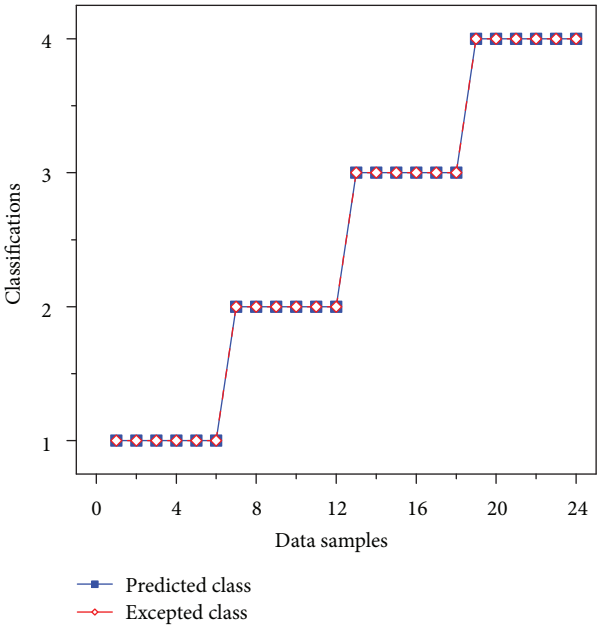

Figure 13: The classifying result of S-Kohonen network.

24 data have been classified correctly; the accuracy is 100%. Therefore, it can be concluded that the proposed MTR method can correctly recognize the bolt loosening location and the recognizing accuracy is extremely high.

5. Conclusion

The problem of detecting bolt loosening for a complicated multibolt-jointed structure is investigated. To this end, a modified time reversal guided wave method is proposed in this paper. Different with the conventional time reversal guided wave method, the response signal due to a tone burst input received at the healthy structure is time reversed and saves as standard reemitting signal. The peak amplitude of the focalized wave packet in the reconstructed signal due to the SRS is extracted as tightness index. By bonding PZT sensors at different joint locations inside the structure, multiple tightness indices can be obtained, where each tightness index presents the correlation between the current joint condition to its healthy condition at the joint. To analyze a large number of tightness indices, a principle component analysis method is introduced, and a neural network-based loosening detection method is proposed.

Experiments at a simulated TPS panel are conducted to verify the feasibility and effectiveness of the MTR method for bolt loosening identification. Different bolt loosening cases are considered, and repeating experiments have been done. Conclusions can be extracted from the analysis of experiment results. It is found that the proposed modified time reversal method can be used to identify and localize the bolt loosening in a simulated TPS panel. By analyzing principal components Y_is, the loosened bracket can be found out. Moreover, the change of TI_i becomes more distinct with the increase of the number of loosening bolt. This work can be extended to similar bolt loosening detection problems in variety multibolt-jointed structures.

Data Availability

The data used to support the findings of this study are available from the corresponding author upon request.

Conflicts of Interest

The authors declare that they have no conflicts of interest.

Acknowledgments

The authors wish to acknowledge the financial support from the China NSAF Project (Grant no. U1530139), China Science Challenge Project (Grant no. TZ2018007), and National Natural Science Foundation of China (Grant no. 51705422).

References

[1] C. R. Farrar and K. Worden, "An introduction to structural health monitoring," *Philosophical Transactions of the Royal Society A Mathematical, Physical and Engineering Sciences*, vol. 365, no. 1851, pp. 303–315, 2010.

[2] R. M. Vandawaker, A. N. Palazotto, and R. G. Cobb, "Damage detection through analysis of modes in a partially constrained plate," *Journal of Aerospace Engineering*, vol. 20, no. 2, pp. 90–96, 2007.

[3] M. D. Todd, J. M. Nichols, C. J. Nichols, and L. N. Virgin, "An assessment of modal property effectiveness in detecting bolted joint degradation: theory and experiment," *Journal of Sound and Vibration*, vol. 275, no. 3–5, pp. 1113–1126, 2004.

[4] M. Mitra and S. Gopalakrishnan, "Guided wave based structural health monitoring: a review," *Smart Materials & Structures*, vol. 25, no. 5, article 053001, 2016.

[5] H. Sohn, C. R. Farrar, and D. J. Inman, "Overview of piezoelectric impedance-based health monitoring and path forward," *The Shock and Vibration Digest*, vol. 35, no. 6, pp. 451–463, 2003.

[6] V. Giurgiutiu, A. Zagrai, and J. B. Jing, "Piezoelectric wafer embedded active sensors for aging aircraft structural health monitoring," *Structural Health Monitoring*, vol. 1, no. 1, pp. 41–61, 2002.

[7] A. V. G. Madhav and S. C. Kiong, "Application of electromechanical impedance technique for engineering structures: review and future issues," *Journal of Intelligent Material Systems and Structures*, vol. 21, no. 1, pp. 41–59, 2010.

[8] D. M. Peairs and D. J. Inman, "Improving accessibility of the impedance-based structural health monitoring method," *Journal of Intelligent Material Systems and Structures*, vol. 15, no. 2, pp. 129–139, 2004.

[9] D. L. Mascarenas, G. Park, K. M. Farinholt, M. D. Todd, and C. R. Farrar, "A low-power wireless sensing device for remote inspection of bolted joints," *Proceedings of the Institution of Mechanical Engineers Part G Journal of Aerospace Engineering*, vol. 223, no. 5, pp. 565–575, 2009.

[10] S. Kuznetsov, I. Pavelko, T. Panidis, V. Pavelko, and I. Ozolinsh, "Bolt-joint structural health monitoring by the method of electromechanical impedance," *Aircraft Engineering and Aerospace Technology: An International Journal*, vol. 86, no. 3, pp. 207–214, 2014.

[11] J. Yang and F. K. Chang, "Detection of bolt loosening in C–C composite thermal protection panels: I. Diagnostic principle," *Smart Materials & Structures*, vol. 15, no. 2, pp. 581–590, 2006.

[12] A. C. Montoya and A. K. Maji, "An assessment of joint rigidity with ultrasonic wave energy," *Journal of Nondestructive Evaluation*, vol. 30, no. 3, pp. 122–129, 2011.

[13] T. Wang, G. Song, Z. Wang, and Y. Li, "Proof-of-concept study of monitoring bolt connection status using a piezoelectric based active sensing method," *Smart Materials & Structures*, vol. 22, no. 8, article 087001, 2013.

[14] D. Doyle, A. Zagrai, B. Arritt, and H. Cakan, "Damage detection in bolted space structures," *Journal of Intelligent Material Systems and Structures*, vol. 21, no. 3, pp. 251–264, 2010.

[15] F. Amerini and M. Meo, "Structural health monitoring of bolted joints using linear and nonlinear acoustic/ultrasound methods," *Structural Health Monitoring*, vol. 10, no. 6, pp. 659–672, 2011.

[16] J. Bao, Y. Shen, and V. Giurgiutiu, "Linear and nonlinear finite element simulation of wave propagation through bolted lap joint," in *54th AIAA/ASME/ASCE/AHS/ASC Structures, Structural Dynamics, and Materials Conference*, pp. 1–12, Boston, MA, USA, 2013.

[17] Y. Shen, J. Bao, and V. Giurgiutiu, "Health monitoring of aerospace bolted lap joints using nonlinear ultrasonic spectroscopy: theory and experiments," *International Workshop on Structural Health Monitoring*, vol. 745, pp. 2333–2340, 2013.

[18] M. Zhang, Y. Shen, L. Xiao, and W. Qu, "Application of subharmonic resonance for the detection of bolted joint looseness," *Nonlinear Dynamics*, vol. 88, no. 3, pp. 1643–1653, 2017.

[19] W. Zhou, Y. Shen, L. Xiao, and W. Qu, "Application of nonlinear-modulation technique for the detection of bolt loosening in frame structure," *Journal of Testing and Evaluation*, vol. 44, no. 2, pp. 967–975, 2016.

[20] Z. Zhang, M. Liu, Z. Su, and Y. Xiao, "Quantitative evaluation of residual torque of a loose bolt based on wave energy dissipation and vibro-acoustic modulation: a comparative study," *Journal of Sound and Vibration*, vol. 383, pp. 156–170, 2016.

[21] C. H. Wang, J. T. Rose, and F. K. Chang, "Computerized time-reversal method for structural health monitoring," in *Proceedings SPIE, Nondestructive Evaluation and Health Monitoring of Aerospace Materials and Composites II*, vol. 5046, no. 2, pp. 48–58, San Diego, CA, USA, August 2003.

[22] H. W. Park, H. Sohn, K. H. Law, and C. R. Farrar, "Time reversal active sensing for health monitoring of a composite plate," *Journal of Sound and Vibration*, vol. 302, no. 1-2, pp. 50–66, 2007.

[23] H. W. Park, S. B. Kim, and H. Sohn, "Understanding a time reversal process in lamb wave propagation," *Wave Motion*, vol. 46, no. 7, pp. 451–467, 2009.

[24] B. Poddar, A. Kumar, M. Mitra, and P. M. Mujumdar, "Time reversibility of a lamb wave for damage detection in a metallic plate," *Smart Materials & Structures*, vol. 20, no. 2, article 025001, 2011.

[25] R. Watkins and R. Jha, "A modified time reversal method for lamb wave based diagnostics of composite structures," *Mechanical Systems & Signal Processing*, vol. 31, no. 8, pp. 345–354, 2012.

[26] S. Mustapha, Y. Lu, J. Li, and L. Ye, "Damage detection in rebar-reinforced concrete beams based on time reversal of guided waves," *Structural Health Monitoring*, vol. 13, no. 4, pp. 347–358, 2014.

[27] S. Mustapha and L. Ye, "Propagation behaviour of guided waves in tapered sandwich structures and debonding identification using time reversal," *Wave Motion*, vol. 57, pp. 154–170, 2015.

[28] S. Mustapha, L. Ye, D. Wang, and Y. Lu, "Debonding detection in composite sandwich structures based on guided waves," *AIAA Journal*, vol. 50, no. 8, pp. 1697–1706, 2012.

[29] W. Tao, L. Shaopeng, S. Junhua, and L. Yourong, "Health monitoring of bolted joints using the time reversal method and piezoelectric transducers," *Smart Materials & Structures*, vol. 25, no. 2, article 025010, 2016.

[30] S. M. Parvasi, S. C. M. Ho, Q. Kong, R. Mousavi, and G. Song, "Real time bolt preload monitoring using piezoceramic transducers and time reversal technique—a numerical study with experimental verification," *Smart Materials & Structures*, vol. 25, no. 8, article 085015, 2016.

[31] A. Zagrai, D. Doyle, and B. Arritt, "Embedded nonlinear ultrasonics for structural health monitoring of satellite joints," in *Proceedings-SPIE, Health Monitoring of Structural and Biological Systems*, vol. 6935, San Diego, CA, USA, March 2008.

[32] N. Kambhatla and T. Leen, "Dimension reduction by local principal component analysis," *Neural Computation*, vol. 9, no. 7, pp. 1493–1516, 1997.

[33] V. Lopes and S. D. Silva, "Structural health monitoring algorithms for smart structures," in *Damage Prognosis: for Aerospace, Civil and Mechanical Systems*, John Wiley & Sons, Ltd., 2005.